

Two-photon Double Ionization of H₂ in Intense Femtosecond Laser PulsesXiaoxu Guan¹, Klaus Bartschat¹, and Barry I. Schneider²¹*Department of Physics and Astronomy, Drake University, Des Moines, Iowa 50311, USA and*²*Physics Division, National Science Foundation, Arlington, Virginia 22230, USA*

(Dated: November 15, 2018)

Triple-differential cross sections for two-photon double ionization of molecular hydrogen are presented for a central photon energy of 30 eV. The calculations are based on a fully *ab initio*, nonperturbative, approach to the time-dependent Schrödinger equation in prolate spheroidal coordinates, discretized by a finite-element discrete-variable-representation. The wave function is propagated in time for a few femtoseconds using the short, iterative Lanczos method to study the correlated response of the two photoelectrons to short, intense laser radiation. The current results often lie in between those of Colgan *et al* [J. Phys. B **41** (2008) 121002] and Morales *et al* [J. Phys. B **41** (2009) 134013]. However, we argue that these individual predictions should not be compared directly to each other, but preferably to experimental data generated under well-defined conditions.

PACS numbers: 33.80.-b, 33.80.Wz, 31.15.A-

Mapping the four-body breakup processes of the hydrogen molecule via multiphoton absorption has recently become feasible experimentally at the free-electron laser facility FLASH. Although the angular distributions and the kinetic-release-energy spectrum of ionic fragments of D₂ were measured [1], determining the angular distribution of the ejected electrons is very difficult. Compared to one-photon double ionization (DI) of H₂ [2, 3], an accurate theoretical description of the two-photon DI of the H₂ molecule is also extremely challenging. Previous calculations by Colgan *et al* [4], who employed the time-dependent close-coupling (TDCC) method, and by Morales *et al* [5], who used a time-independent exterior complex scaling (ECS) treatment, showed considerable disagreements regarding both the shape and the magnitude of the predicted triple differential cross section (TDCS). However, both predicted a strong dependence of the angular distribution of the ejected electrons on the alignment angle between the linear laser polarization vector (ϵ) and the molecular axis (ς).

The discrepancies between the previous, computationally very demanding calculations provided the primary motivation for the present project. We emphasize, however, that these calculations were performed for much different conditions. Colgan *et al* [4] used a femtosecond laser pulse with a peak laser intensity of 10^{15} W/cm² that could lead to serious depletion of the ground state and *may* not be in the perturbative regime. The calculation of Morales *et al* [5] was for a well-defined photon energy and is equivalent to a weak pulse of near infinite duration. In light of the ongoing discussions, it seemed important to perform another independent calculation to investigate the similarities and differences in the results and to understand their origin. Consequently, we also consider the two-photon DI of the H₂ molecule in the parallel and perpendicular geometries at an incident photon energy centered around 30 eV and equal sharing of the excess energy. Our pulse (see details below) lies in the perturbative regime but, like the TDCC model, has a bandwidth

that may access doubly excited electronic states in the H₂ spectrum unavailable to Morales *et al*. The effect of such states on the outcome of a short-pulse experiment is not known at this time. The details could be highly complex, and a theoretical treatment may ultimately have to go beyond the current model.

The two-center nature of H₂ already destroys the spherical symmetry of the problem even in the absence of an external laser field. While it is numerically feasible to carry out the calculations in a spherical coordinate system at the center of the H₂ molecule, this becomes more and more difficult for heavier diatomics due to the slow convergence of the multi-center electron-nuclear interaction. Fortunately, the prolate spheroidal coordinate system offers an attractive alternative for diatomics [6], since the electron-nuclear interaction is rendered benign.

The addition of an external field causes a symmetry reduction when the laser field is not parallel to the internuclear axis. Compared to the atomic He target, therefore, the situation in this simplest two-electron molecule is complicated due to an additional degree of freedom, namely the alignment angle between the ϵ - and ς -axes. While the emission modes of photoelectrons from atomic targets exhibit rotational symmetry with respect to the polarization vector, this may no longer be the case for an arbitrary $\epsilon - \varsigma$ geometry. All of these issues conspire to make the response of the H₂ molecule to temporal laser fields much more computationally demanding than the two-photon DI of the helium atom.

For the frozen-nuclei approximation used here and in [4, 5] to be physically meaningful, the time scale for ionization by the field has to be much shorter than the characteristic time of the nuclear motion. For *direct*, rather than *sequential* double ionization, this condition is fulfilled here, since the *simultaneously* ejected electrons have a speed over ten times larger than what the protons can achieve in the subsequent Coulomb explosion. For a central photon energy of 30 eV, we expose the H₂ molecule to a 10-cycle sine-squared laser pulse at a peak

intensity of 10^{14} W/cm², followed by a 2-cycle field-free evolution. This “10 + 2”-cycle takes about 1.6 fs, which is sufficiently long to extract a well-defined cross section in the perturbative regime of relatively low peak intensities. Nevertheless, a comparison with results from time-independent calculations is *not* directly possible, due to the energy width of several eV.

Our treatment of the six-dimensional time-dependent Schrödinger equation (TDSE) of the laser-driven H₂ molecule relies on the *two-center* prolate spheroidal coordinates (ξ, η, φ) . The ranges of the variables are $\xi \in [1, +\infty)$, $\eta \in [-1, +1]$, and $\varphi \in [0, 2\pi]$. For the temporal laser field $\mathbf{E}(t) = \epsilon E(t)$, the TDSE in the dipole length gauge reads

$$i \frac{\partial}{\partial t} \Psi(1, 2, t) = \left[\mathcal{H}_1 + \mathcal{H}_2 + \frac{1}{r_{12}} + \mathbf{E}(t) \cdot (\mathbf{r}_1 + \mathbf{r}_2) \right] \Psi(1, 2, t). \quad (1)$$

Here \mathcal{H}_i represents the field-free single-electron Hamiltonian for electron “*i*” while \mathbf{r}_i is its coordinate, measured relative to the center of the molecule. As usual, $r_{12} = |\mathbf{r}_1 - \mathbf{r}_2|$.

We expand the H₂ wave function in the body-frame as

$$\Psi(1, 2, t) = \frac{1}{2\pi} \sum_{m_1 m_2} \Pi_{m_1 m_2}(\xi_1, \eta_1, \xi_2, \eta_2, t) e^{i(m_1 \varphi_1 + m_2 \varphi_2)}, \quad (2)$$

where m_1 and m_2 denote the magnetic quantum numbers of the two electrons along the molecular axis. To discretize this partial differential equation, we employ the finite-element discrete-variable-representation (FEDVR) approach for the (ξ, η) variables [6]. Thus $\Pi_{m_1 m_2}(\xi_1, \eta_1, \xi_2, \eta_2, t)$ is expanded in a product of “radial” $\{f_i(\xi)\}$ and “angular” $\{g_k(\eta)\}$ DVR functions. The notation originates from the asymptotic behavior of $\xi \rightarrow 2r/R$ and $\eta \rightarrow \cos\theta$ in spherical coordinates, when the electron is far away from the nuclei.

To treat the electron-electron interaction we employ the Neumann expansion of $1/r_{12}$ in prolate spheroidal coordinates [7],

$$\frac{1}{r_{12}} = \frac{2}{R} \sum_{\ell=0}^{\infty} \sum_{m=-\ell}^{\ell} (-1)^{|m|} (2\ell + 1) \left(\frac{(\ell - |m|)!}{(\ell + |m|)!} \right)^2 \quad (3)$$

$$\times P_{\ell}^{|m|}(\xi_{<}) Q_{\ell}^{|m|}(\xi_{>}) P_{\ell}^{|m|}(\eta_1) P_{\ell}^{|m|}(\eta_2) e^{im(\varphi_1 - \varphi_2)}.$$

Here $\xi_{>}$ and $\xi_{<}$ are the larger and smaller of ξ_1 and ξ_2 , respectively. $P_{\ell}^{|m|}(\xi)$ and $Q_{\ell}^{|m|}(\xi)$ are regular and irregular Legendre functions defined for $\xi \in (1, +\infty)$, while $P_{\ell}^{|m|}(\eta)$ is specified for $\eta \in [-1, +1]$. By suitably generalizing the approach used in [8] for the spherical case, it is possible to reformulate the computation of the required matrix elements of the operator in Eq. (3) as the solution of a two-center Poisson equation. This results in a diagonal representation of the matrix elements of the electron-electron Coulomb interaction and considerably simplifies the FE-DVR discretization procedure.

The time-dependent electron wave packets of the laser-driven H₂ molecule were generated by using our recently

developed Arnoldi-Lanczos algorithm on the DVR mesh points [9]. Compared to the treatment of atomic targets in spherical coordinates, however, the boundary conditions in spheroidal coordinates require further elaboration. As demonstrated in [6], the “radial” and “angular” functions are not simple polynomials for odd $|m|$. Special attention must be paid to the square-root asymptotics as $\xi \rightarrow 1$ (from above) and $|\eta| \rightarrow 1$ (from below) when $|m|$ is odd. By introducing the factors $\sqrt{\xi^2 - 1}$ and $\sqrt{1 - \eta^2}$, respectively, in the DVR bases $f_i(\xi)$ and $g_k(\eta)$ for odd $|m|$ to account for the behavior near the boundary, it is possible to use a single quadrature for all m .

A spatial box with $\xi_{\max} = 100$ was set up to truncate the configuration space. Solving the TDSE in imaginary time with a grid of $N_{\xi} \times N_{\eta} = 224 \times 9$ and $|m|_{\max} = |m_1|_{\max} = |m_2|_{\max} = 3$, we obtained the electronic energy of the initial $X^1\Sigma_g^+$ state at the internuclear distance of $R = 1.4 a_0$ ($a_0 = 0.529 \times 10^{-10}$ m denotes the Bohr radius) as -1.8873 atomic units (a.u.), in good agreement with the recent benchmark value of -1.888761428 a.u. by Sims and Hagstrom [10] (after taking out the nucleus-nucleus interaction of $1/1.4$). This yields a double-ionization threshold of 51.4 eV above the initial electronic state.

To calculate the angle-resolved differential cross sections, we project the wave packet at the end of the time propagation onto uncorrelated two-electron continuum states, which are approximately constructed in terms of the single-electron continuum states of the H₂⁺ ion. For a momentum k , the “radial” part of the continuum state, $T_{|m|q}^{(k)}(\xi)$, behaves asymptotically as

$$T_{|m|q}^{(k)}(\xi) \xrightarrow{\xi \rightarrow \infty} \frac{1}{\xi R} \sqrt{\frac{8}{\pi}} \sin \left(c\xi + \frac{a}{2c} \ln(2c\xi) - \frac{\ell\pi}{2} + \Delta_{|m|q}(k) \right). \quad (4)$$

Here $\Delta_{|m|q}(k)$ is the two-center Coulomb phase shift, $c = kR/2$, $a = 2R$, and $\ell = |m| + q$ for the H₂⁺ ion. In addition to $|m|$, an integer q , which is the number of nodes of the angular function, is used to label the continuum state. In the unified-atom limit, $R \rightarrow 0$, the above two-center radial function reduces to the well-known atomic Coulomb wave function.

Let us comment again on the similarities and the differences between the various approaches. One might expect our calculation to yield similar results to the TDCC model, although our numerical implementation is very different from that of Colgan *et al* [4]. For example, they used a finite-difference method and a flat-top pulse with 12-cycle time duration at a much stronger intensity of 10^{15} W/cm². Most importantly, however, both models project onto uncorrelated Coulomb functions.

In the ECS approach of Morales *et al* [5], on the other hand, the information was extracted from a time-independent wave function, which effectively corresponds to an infinite propagation time. The complicated three-body correlated Coulomb boundary condition is avoided in this approach. We would best simulate the ECS model by exposing the H₂ molecule to a weaker light field with a

longer pulse duration, and also by propagating for a long time after the external field has died off. Then the electrons have moved very far away from the nuclei and the projection to uncorrelated functions is increasingly appropriate [11]. Since this would require a large amount of computational resources, we decided on the compromise of testing our procedure by varying the number of field-free propagation cycles between one and three. We only noticed a small sensitivity to the time of projection, and hence are confident that our results are converged to a few percent. In addition, it should be noted that TDCC and ECS results for one-photon DI [2, 3], performed with similar philosophies of extracting the information, showed excellent agreement with each other.

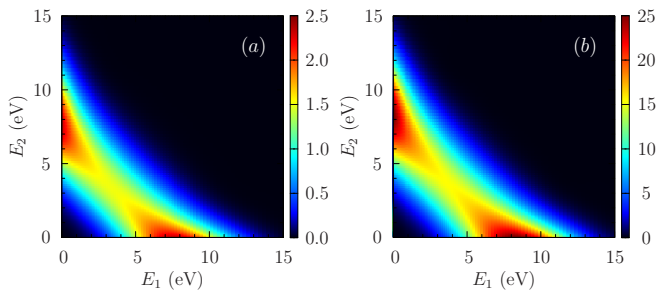


FIG. 1. (Color online) Energy probability distribution of two ejected electrons in the parallel (a) and perpendicular (b) geometries for a sine-squared laser pulse of 10 optical cycles, a central energy of 30 eV, and a peak intensity of 10^{14} W/cm². The color bars correspond to multiples of 10^{-7} eV⁻². Note the different scales in the two panels.

Figure 1 depicts the correlated energy distributions of the two ejected electrons after two-photon absorption. As they are similar in shape for the both parallel and the perpendicular geometries, information about any possibly preferred direction of the outgoing electrons is smeared out in the energy distributions. Figure 1 reveals, however, that the probability of two-photon DI in the perpendicular geometry is about ten times larger than for the parallel case, in qualitative agreement with the findings of [4].

Next we explore the angle-resolved cross sections in a particular plane, namely that formed by the molecular axis and the laser polarization axis, a coplanar configuration. Note that the angles of the two ejected electrons, θ_1 and θ_2 , are measured with respect to the ϵ vector rather than the ζ axis.

Our TDCS results for the parallel geometry are shown in Fig. 2. They did not change within the thickness of the lines when an enlarged spatial box of $\xi_{\max} = 150$ was used. They are numerically converged at $|m|_{\max} = 5$ (see the convergence checks below). Near the maximum of the TDCS, the time-independent ECS results are significantly larger than the present FE-DVR and TDCC predictions. The present TDCS results for the parallel geometry are approximately three times smaller than those of Morales *et al* [5], but twice as large as those of

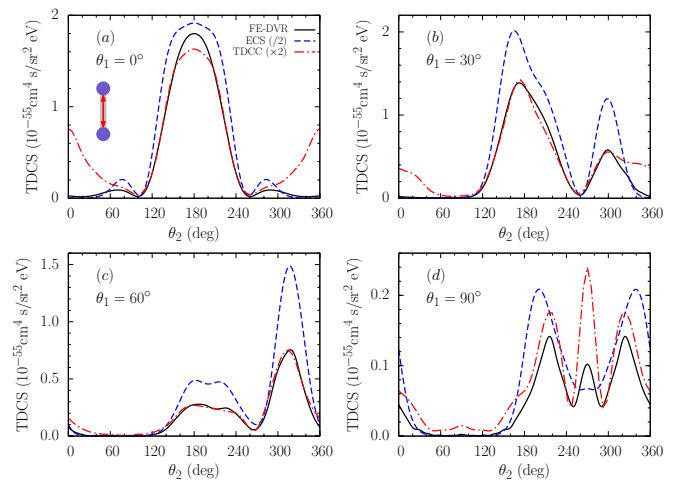


FIG. 2. (Color online) Coplanar TDCS for two-photon DI of H₂ at equal energy sharing ($E_1 = E_2 = 4.3$ eV) of the two ejected electrons in the parallel geometry. The laser parameters are the same as in Fig. 1. Also shown are the TDCC results of Colgan *et al* [4] and the ECS results of Morales *et al* [5], multiplied by the scaling factors indicated in the legend. The definition of the TDCS is consistent in all three calculations.

Colgan *et al* [4], i.e., they generally lie in between the previous predictions. This is indicated by the scaling factors shown in the legend.

The various sets of results disagree in the predicted magnitude as well as in the shape of the angular dependence. A prominent difference concerns the “wing” structures of nonvanishing TDCS values near $\theta_2 \simeq 0^\circ$ and 360° for $\theta_1 = 0^\circ$ and 30° observed in Ref. [4]. In addition to the dominant back-to-back escape mode, there is a noticeable forward emission in the prediction of Colgan *et al*. This counter-intuitive forward-to-forward escape mode for two electrons carrying the same kinetic energy and traveling in the same direction is not supported by either the ECS or the present FE-DVR calculations.

Figure 3 displays the corresponding TDCSs for the perpendicular orientation. Here the situation is different from the previous case. Although the ECS results [5] are generally larger than the present and the TDCC predictions [4], they are of similar magnitude. The agreement between the FE-DVR and TDCC calculations is quite satisfactory in this case. In contrast to the parallel geometry, the shapes of the angular distributions in the perpendicular geometry are much closer to those obtained for the helium atom at 42 eV [9].

The TDCS for orientation of the molecular axis parallel to the polarization vector exhibits the molecular effect to the largest extent. Only the $^1\Sigma_g \rightarrow ^1\Sigma_u \rightarrow ^1\Sigma_g$ path of transitions is open in this geometry, because the total magnetic quantum number along the ζ -axis must be conserved. The final state, therefore, has the same symmetry as the initial state. At a right angle between the ϵ - and ζ -axes, on the other hand, the two electrons may be ionized through $^1\Sigma_g \rightarrow ^1\Pi_u \rightarrow ^1\Sigma_g$ or $^1\Sigma_g \rightarrow ^1\Pi_u \rightarrow ^1\Delta_g$, since

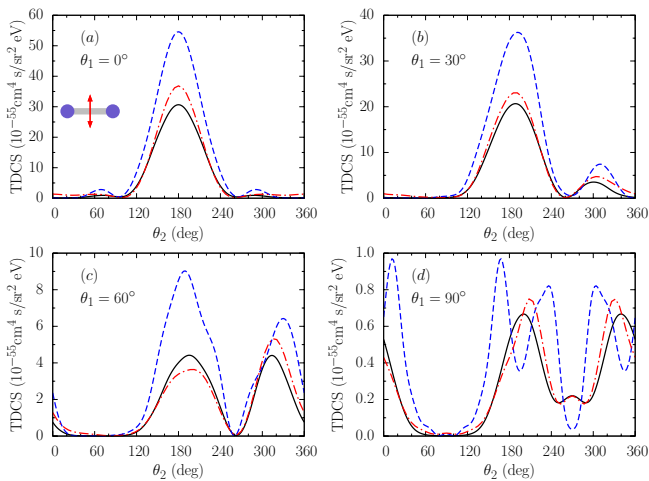


FIG. 3. (Color online) Same as Fig. 2 for the perpendicular geometry. No scaling factors were applied to compare the various predictions.

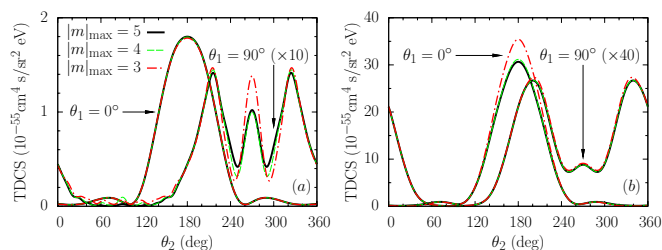


FIG. 4. (Color online) Convergence of the TDCS predictions with increasing $|m|_{\max}$ for the parallel (a) and perpendicular (b) geometry. The results for $|m|_{\max} = 4$ and 5 are hard to distinguish. The laser parameters are the same as in Fig. 2.

the selection rule here is $|\Delta M| = 1$ instead of $|\Delta M| = 0$ (here $M = m_1 + m_2$ is the total magnetic quantum number along the ζ -axis). This is qualitatively similar to those of the atomic target through $^1S^e \rightarrow ^1P^o \rightarrow ^1S^e$ or $^1S^e \rightarrow ^1P^o \rightarrow ^1D^e$. An interference effect between the open channels $^1\Sigma_g$ and $^1\Delta_g$ in H_2 is evident, as it is in the helium atom between the $^1S^e$ and $^1D^e$ channels [12]. Such interference cannot be observed in the parallel orientation, where only one channel is open.

We also performed extensive convergence checks by increasing $|m|_{\max}$ from 3 to 5. Figure 4 shows the convergence for the fixed electron angles of $\theta_1 = 0^\circ$ and $\theta_1 = 90^\circ$. In the parallel case, the TDCS calculated with $|m|_{\max} = 3$ at $\theta_1 = 0^\circ$ is already fully converged, but for $\theta_1 = 90^\circ$ $|m|_{\max} = 5$ is required to obtain essentially converged results. In the perpendicular case, on the hand, the TDCS at $\theta_1 = 0^\circ$ is very sensitive to the value of $|m|_{\max}$, until it stabilizes at $|m|_{\max} = 5$, while the TDCS at $\theta_1 = 90^\circ$ is less sensitive to the choice of $|m|_{\max}$.

Although the parallel and perpendicular orientations exhibit different convergence patterns in terms of θ_1 and θ_2 , we observe that the TDCSs in both geometries behave similarly when we transfer the result to the molecular frame. In that frame, when the fixed electron is measured in the direction perpendicular to the molecular axis, the back-to-back escape mode is most sensitive to the $|m|$ value. When one electron is detected along the molecular axis, the back-to-back mode is the most stable.

In summary, we calculated the two-photon DI of the H_2 molecule by an intense femtosecond laser pulse. Our TDCS results are generally closer to the predictions from the TDCC than from the ECS approach, except for the small-angle behavior in the parallel geometry, where we do not see what seems to be an unphysical increase of the TDCS. A magnitude difference of about a factor of two, rather than five [5], remains in the parallel case. Once again, however, we emphasize that a straight comparison of these results is inappropriate. Great care should be taken when such a comparison is made, particularly when experimental data become available. Knowing the details of the experimental setup will be essential. We plan to extend our present treatment to angular distributions in more general cases with an arbitrary alignment angle between the polarization vector and the molecular axis, and to further study the sensitivity of the theoretical predictions on the details of the pulse.

We are greatly indebted to Prof. F. Martín for providing constructive remarks to improve the manuscript. We also thank Drs. J. Colgan and F. Morales for sending their results in numerical form and helpful discussions. This work was supported by the NSF under grant PHY-0757755 (XG and KB) and supercomputer resources through the Teragrid allocation TG-PHY090031.

[1] Y. H. Jiang *et al*, Phys. Rev. A **81**, 021401(R) (2010).
 [2] W. Vanroose *et al*, Phys. Rev. A **74**, 052702 (2006).
 [3] J. Colgan, M. S. Pindzola, F. Robicheaux, Phys. Rev. Lett. **98**, 153001 (2007).
 [4] J. Colgan, M. S. Pindzola, and F. Robicheaux, J. Phys. B **41**, 121002 (2008); J. Colgan, private communication (2010).
 [5] F. Morales *et al*, J. Phys. B **42**, 134013 (2009).
 [6] L. Tao, C. W. McCurdy, and T. N. Rescigno, Phys. Rev. A **79**, 012719 (2009).
 [7] P. M. Morse and H. Feshbach, in *Methods of Theoretical*

Physics, Parts I and II (McGraw-Hill, 1953).
 [8] C. W. McCurdy, M. Baertschy, and T. N. Rescigno, J. Phys. B **37**, R137 (2004).
 [9] X. Guan, K. Bartschat, and B. I. Schneider, Phys. Rev. A **77**, 043421 (2008).
 [10] J. Sims and S. Hagstrom, J. Chem. Phys. **124**, 094101 (2006).
 [11] L. B. Madsen *et al*, Phys. Rev. A **76**, 063407 (2007).
 [12] S. X. Hu, J. Colgan, and L. A. Collins, J. Phys. B **38**, L35 (2005).